Poly(ethylene terephthalate) Foams: Correlation Between the Polymer Properties and the Foaming Process

L. Sorrentino,[1] E. Di Maio,[2] S. Iannace[1]

[1]*Institute for Composite and Biomedical Materials, National Research Council, Piazzale Enrico Fermi 1, I-80055 Portici, Italy*
[2]*Department of Materials and Production Engineering, University of Naples Federico II, Piazzale Enrico Tecchio 80, I-80125 Napoli, Italy*

ABSTRACT: The foamability of two food-grade, high-molecular-weight poly(ethylene terephthalate)s (PETs) was investigated. Sorption tests were performed to determine the solubility and diffusivity of N_2 and CO_2 in molten polymers at 250°C with a magnetic suspension balance. Pressure-volume-temperature (pVT) data were also measured and used in the context of the Sanchez–Lacombe equation of state to predict the sorption isotherms. The thermal properties, in terms of the glass-transition, melting, and crystallization temperatures, were measured by differential scanning calorimetry analysis on the two high-molecular-weight PETs and, for comparison, on a bottle-grade PET. The rheological properties were measured to asses the improvement of the high-molecular-weight PET with respect to the bottle-grade one. Expansion tests were performed on the two high-molecular-weight grades and bottle-grade PETs with a batch foaming process with N_2, CO_2, and an 80–20 wt % N_2–CO_2 mixture used as blowing agents. The whole processing window was explored in terms of temperature, pressure drop rate, and saturation pressure. The results of the foaming experiments were correlated to gas sorption and the thermal and rheological properties of the polymers in the molten state. The results proved the feasibility of foam processing these two high-molecular-weight grades, which gave, when compared to the bottle grade at specific foaming conditions, very low densities and fine morphologies. © 2009 Wiley Periodicals, Inc. J Appl Polym Sci 116: 27–35, 2010

Key words: blowing agents; macroporous polymers; morphology; polyesters; processing

INTRODUCTION

Poly(ethylene terephthalate) (PET) is a low-cost engineering polymer with good mechanical and thermal characteristics and exhibits high elastic moduli, high glass-transition temperature (T_g), and good crystallinity and solvent resistance.[1] The availability of foams based on PET could be very interesting, mainly for the temperature range allowed by the high melting temperature (T_m) of the bulk polymer and its crystallinity. Such foams can be used in applications such as packaging, thermal insulating panels, and cores for sandwich structures.

However, the low shear and elongational viscosities and low melt strength of conventional PET prevents from being easily foamed by typical technologies such as gas extrusion foaming, and complex procedures have to be used (see, e.g., ref. 2). Different treatments have been developed to improve the PET macromolecular characteristics, in particular, to extend the polymer chain length. In fact, the molecular weight increase, through chain extension or branching, is responsible for the increases in both viscosity and melt strength; these, in turn, facilitate the production of expanded structures.

Among the different solutions proposed, the most cost effective has been the use of epoxy-based[3,4] or dianhydride-based[5] products as chain extenders, to be used during the extrusion foaming process (reactive extrusion). Chain extension is able to strongly increase the polymer viscosity at low strain rates. In particular, in the study in ref.[6], the addiction of pyromellitic dianhydride (PMDA) was used in a reactive extrusion process on low-molecular-weight PET to raise the polymer viscosity by the joining of the ─OH end groups of the macromolecules. Because of the high temperature involved in this process and despite the ease of the process, reactive extrusion was not able to guarantee a constant and controlled level of chain extension or weight-average molecular weight/number-average molecular weight ratio without the introduction of branching or gel formation.[5,7]

A more accurate process was patented by Cobarr SpA and included the fast melt mixing of PET and PMDA (to prevent degradations and/or reactions) followed by a postcondensation step at temperature quite below T_m. The molecular weight was controlled by the variation of the postcondensation temperature, PMDA content, and processing time.[8,9]

Correspondence to: L. Sorrentino (luigi.sorrentino@cnr.it).
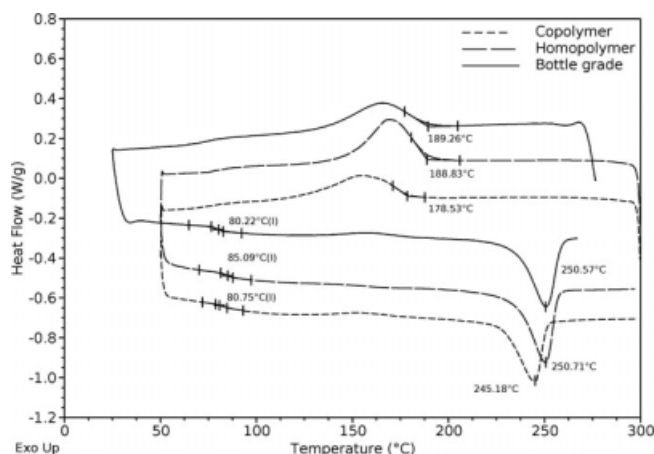
Figure 1 DSC heating and cooling scans of different grades of PET obtained from the DSC analyzer.

In the past, PET microcellular foams have been produced by a two-stage process, generally referred to as a *temperature rise process:* the gas, mainly CO_2, at several 10s of bars, was (1) first solubilized in a thin sheet of PET and (b) subsequently dipped in a high-temperature oil bath for some seconds.[10–12] However, this technique is time consuming and not scalable to continuous processing. The availability of high-molecular-weight linear PET has given rise to many studies on the foaming process, most of them focused on the use of CO_2 or HFC as physical blowing agents, whereas very few works are available on the use of N_2 and CO_2/N_2 mixtures.

In this study, we produced high-molecular-weight PET foams, where chain extension was obtained according to patents[8,9] by the pressure quench method with N_2, CO_2, and their 80/20 mixture as blowing agents.

EXPERIMENTAL

The polymers used for the experiments were commercial-grade, high-molecular-weight PETs with intrinsic viscosities of 1.25 dL/g. Two grades were used: the copolymer, Cobifoam 2 (CF2), differed from the homopolymer, Cobifoam 0 (CF0), by a small amount of isophthalic acid. This induced lower degrees of crystallinity and macromolecular structure order, whose effects were not minor. The bottle-grade PET (BG), used for comparison, exhibited an intrinsic viscosity of 0.78 dL/g. All PETs were kindly supplied by the COBARR SpA Mossi & Ghisolfi Group (Tortona, Italy).

The polymers were characterized by differential scanning calorimetry (DSC) with a TA Instruments DSC model 2920 (New Castle, DE) to evaluate the crystallization temperatures from the melt state to roughly estimate the lower end of the foaming temperature range. A double-scan procedure (heating–cooling–heating) was performed on the samples

from 30 to 300°C at a heating rate of 10°C/min after the samples were vacuum-dried overnight at 120°C. Some nonisothermal DSC tests were performed from the melt state, with a cooling rate ranging from 2 to 20°C/min, to compare the crystallization kinetics of the two high-molecular PETs.

Rheological tests were performed with an ARES rheometer from Rheometric Scientific (now TA Instruments, New Castle, DE) to compare the viscosities of all of the polymer samples at temperatures from 280 to 310°C in the frequency range between 0.1 and 10 Hz.

The pressure-volume-temperature (pVT) behavior of the PETs was evaluated through isothermal measurements at pressures up to 200 MPa and temperatures from 25 to 320°C in a GNOMIX high pressure dilatometer (Boulder, CO). Measurements were performed with the classical bellows technique, in which pressure was applied to the samples through a confining fluid, mercury, and the volume was measured by a linear variable differential transformer (LVDT) mounted beneath the pressure vessel. The measurements procedure was described in detail elsewhere.[13]

A magnetic suspension balance (Rubotherm ISOSORP, Bochum, Germany, maximum weight = 100 g, resolution = 10 µg) was used to evaluate the sorption of CO_2 and N_2 in PET and to measure the CO_2/PET and N_2/PET mutual diffusivities in the PET molten state (at 250°C after being pretreated at 300°C). In the experiment, a crucible containing the polymer sample was attached to a permanent magnet, and the system was placed in a sorption chamber maintained at a controlled temperature (± 0.05°C). The system could withstand pressures up to 13 MPa. The permanent magnet was kept suspended by an electromagnet, which was attached to the hook of an analytical balance (model MC 5 from Sartorius, Goettingen, Germany). Coupling
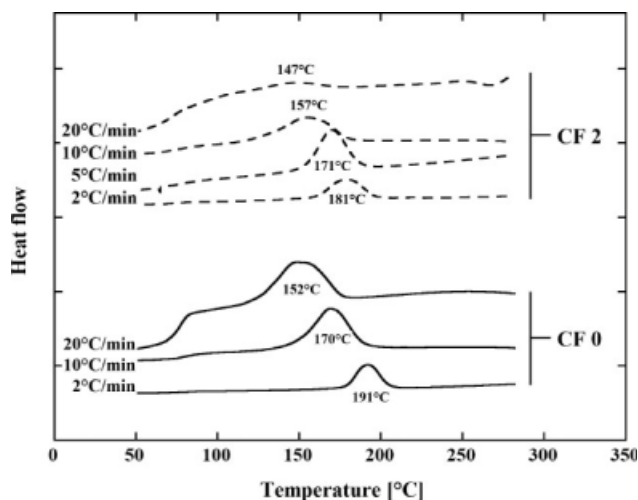
Figure 2 Effect of the cooling rate on the crystallization peaks during the cooling ramp from the melt state.
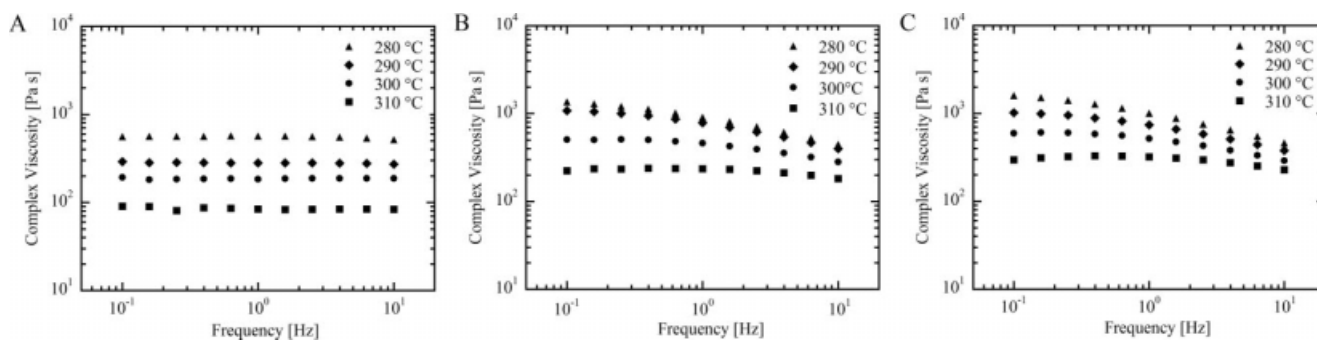
Figure 3 Complex viscosity of (A) bottle-grade PET, (B) CF0, and (C) CF2 as function of temperature.

between the magnet and the electromagnet was electronically controlled. The balance and the electromagnet were completely isolated from the sorption chamber and maintained at ambient conditions. The force change due to mass uptake during the sorption process was transmitted from the sorption chamber to the analytical balance by the coupling of the permanent magnet and electromagnet. We conducted the measurements by performing step-change sorption experiments. Consecutive sorption tests were conducted by step increments of the carbon dioxide and nitrogen pressure (ca. 0.3-MPa steps) with preheated gas, after the attainment of the equilibrium weight in the previous step.

All foam samples were produced by the expansion of about 0.5 g of polymer in a pressure vessel with a batch process. Before each test, the PET pellets were vacuum-dried overnight at 120°C. Two samples for each PET grade were enclosed in the pressure vessel at room temperature. Then, a vacuum pump was used for 15 min before gas injection to assure the absence of air (humidity, mainly) in the batch internal volume. The selected gas (CO_2, N_2, or their 20/80 wt % mixture) was then inserted into the vessel at the desired pressure [90 bar (LP) and 160 bar (HP)], and then, the temperature was raised to and kept at 300°C for 35 min to erase

the previous thermal history. This temperature was selected as the minimum T_m of the perfect PET crystal, according to a procedure described elsewhere.[14] After this step, solubilization was conducted at 250°C for 30 min. At the end of solubilization, the temperature was lowered to the desired value (ranging from 180 to 250°C), and then, the pressure was quenched to room pressure in a controlled manner.

All samples were qualitatively evaluated and, where applicable, the density of foamed samples was measured with a hydrostatic balance according to ASTM D 792. The morphological characteristics (mean cell diameter and cell number density) were measured by analysis of sample micrographs obtained with an optical stereomicroscope (model Z16APO, Leica Microsystems GmbH, Wetzlar, Germany) and a scanning electron microscope (model S440, Leica Microsystems GmbH) with ImageJ software (National Institutes of Health (NIH), Bethesda, MD).

RESULTS AND DISCUSSION

Thermal analysis

As evidenced by the DSC diagrams shown in Figure 1, the CF0 sample exhibited a T_g of 85°C and a T_m of 251°C. The peak temperature of the dynamic crystallization from the molten state was 169°C, whereas the onset temperature was 190°C. The CF2 sample exhibited a T_g of 81°C and a T_m of 245°C, whereas the onset and peak temperatures of crystallization from the molten state were 180 and 154°C, respectively. The onset temperatures for crystallization
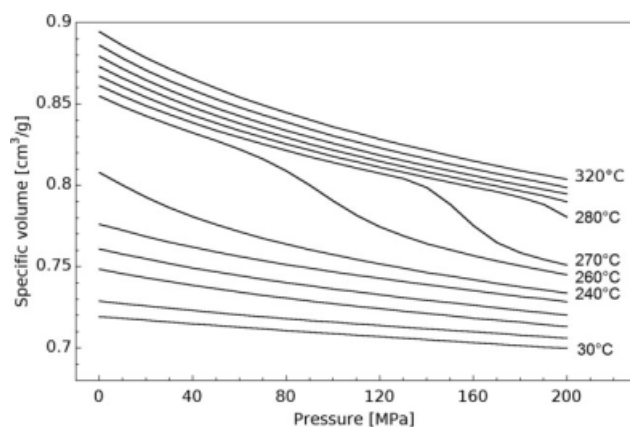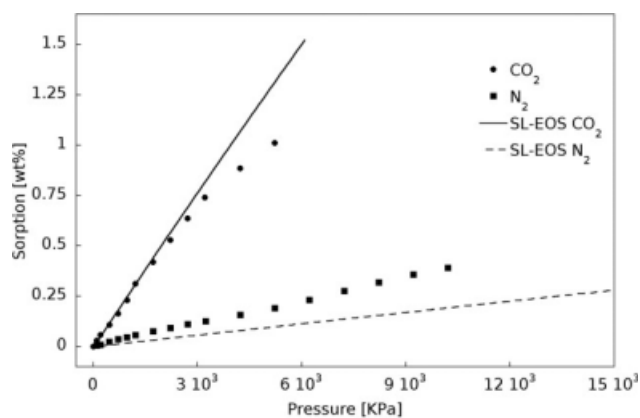

Figure 4 pVT data for CF0.

TABLE I
SL–EOS Characteristic Parameters for the Different Materials Used in This Study

| Material	ρ^* (cm^3/g)	T^* (K)	P^* (atm)	References
PET BG	1409	761	7166	16 and 17
PET CF0	1380	767	6910	This study
PET CF2	1380	768	6697	This study
CO_2	1605	3043	923	18 and 19
N_2	1100	1645	537	18 and 19

ρ^* is the characteristic density.

Figure 5 Sorption isotherms of CO_2 and N_2 at 250°C in CF0 and the SL–EOS model predictions ($\psi = 1$).

were considered to be the lower end values for the foaming temperature range. The DSC scan of the bottle-grade PET is also shown for comparison purposes. As evidenced in ref. 14, the foam-grade PET CF0 was characterized by slower crystallization kinetics compared to the bottle-grade PET.

In Figure 2, the comparison of the crystallization temperature peaks for different cooling rates is presented for the different polymers. The use of a higher cooling rate strongly reduced the onset of the crystallization temperature from the melt state. Furthermore, CF2 clearly exhibited slower crystallization kinetics compared to CF0.

Rheological characterization

Both foam-grade PETs exhibited shear thinning behavior at the higher end of the measured frequency range and Newtonian behavior at low shear rates [Fig. 3(A–C)], but in all of the conditions, the bottle-grade PET viscosity was significantly lower (ca. one fourth of the foam-grade polymer) at the same temperature. The measured viscosity, with
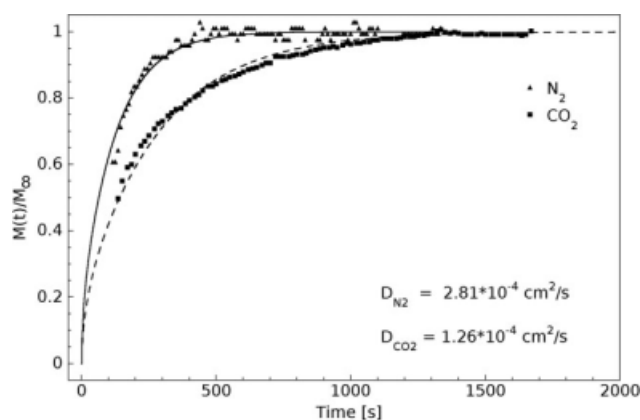
Figure 6 Sorption kinetics of CO_2 and N_2 in PET. M(t), M_∞, D_{N2}, D_{CO2} are the amount of gas absorbed at time t and at equilibrium, and the diffusivity of N_2 and CO_2, respectively.

TABLE II
Processing Conditions for the Polymers

| Gas type	CO_2, N_2, and an 80/20 wt % N_2/CO_2 mixture
T_m	300°C
Solubilization	35 min at 250°
Foaming temperatures	From 180 to 250°C with steps of 10°C
Solubilization pressure	90 bar (LP) and 160 bar (HP)

respect to the bottle-grade PET, proved the increased weight-average molecular weight of CF0 and CF2, and this enhancement will be useful for foam stabilization,[15] as observed in the following foaming experiments.

pVT characterization

As an example, Figure 4 reports the pVT data of CF0. The data show the specific volume of the material versus pressure at different temperatures. Both melting in the region 240–300°C at the different pressures and the pressure-induced crystallization are evident. Data collected for the different PETs in the
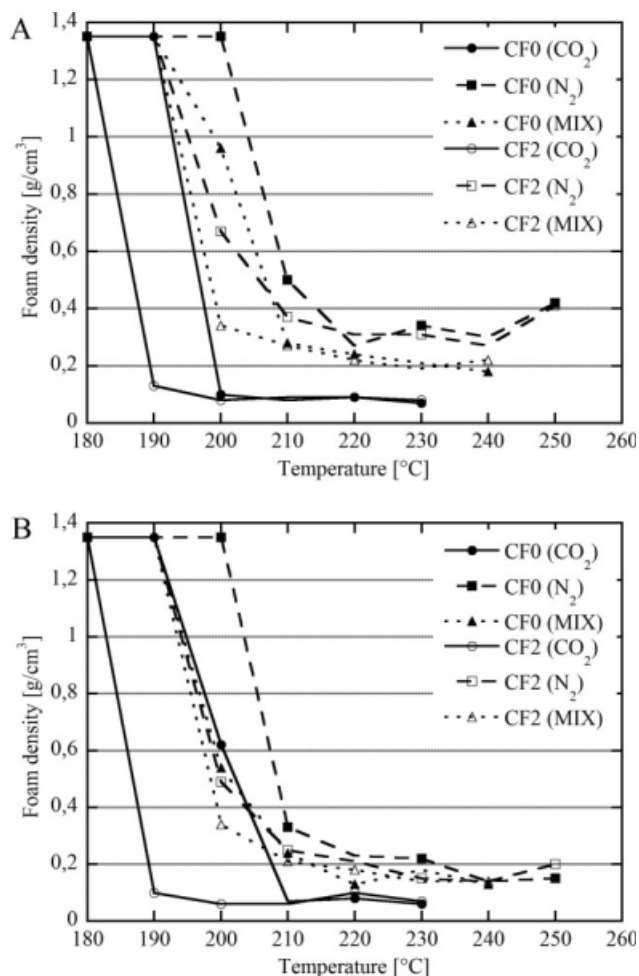
Figure 7 Effect of (A) low and (B) high gas solubilization pressure on the sample densities.
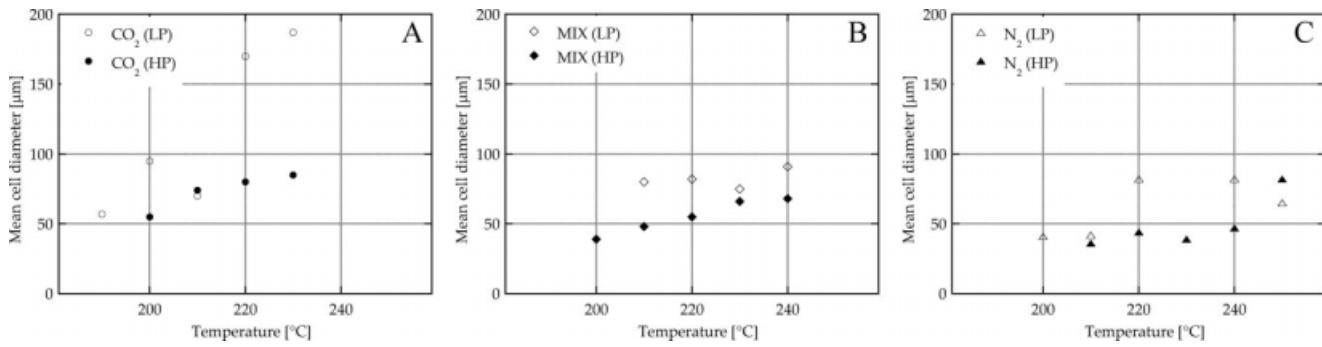
Figure 8 Mean cell diameter of the samples as function of temperature, gas type, and solubilization pressure for the CF0 polymer.

molten state were then used in the context of the Sanchez–Lacombe equation of state (SL–EOS)[16,17] to evaluate the characteristic parameters, reported in Table I for the different polymers. Table I also reports literature data for the characteristic parameters of the blowing agents used in this study. The SL–EOS has the following expression:

$$\tilde{\rho}^2 + \tilde{P} + \tilde{T}\left[\ln(1-\tilde{\rho}) + \left(1-\frac{1}{r}\right)\tilde{\rho}\right] = 0$$

where r is the number of lattice sites occupied by a molecule of fluid and $\tilde{P}$, $\tilde{T}$, and $\tilde{\rho}$ are the reduced parameters (pressure, temperature, and density, respectively) defined as follows:

$$\tilde{P} = \frac{P}{P^*}$$

$$\tilde{T} = \frac{T}{T^*}$$

$$\tilde{v} = \frac{V}{V^*} = \frac{1}{\tilde{\rho}}$$

where P, T, and V are the actual pressure, temperature and volume, respectively, and P^*, T^*, and V^* are the characteristic pressure, temperature and volume, respectively, of the fluid.

To determine the characteristic parameters of the pure polymer and pure gas, it was sufficient to fit the experimental data in terms of reduced parameters with the SL–EOS.

Sanchez and Lacombe extended their theory to the case of mixtures by adopting appropriate mixing rules. The equation of state (EOS) of the mixture is formally identical to the EOS of a pure fluid:[17]

$$\tilde{\rho} = 1 - \exp\left[-\frac{\tilde{\rho}^2}{\tilde{T}} - \frac{\tilde{P}}{\tilde{T}} - \left(1 - \frac{\phi_1}{r_1}\right)\tilde{\rho}\right]$$

where r_1 and ϕ_1 are related to the number of lattice sites and the weight fraction of the gas in the polymer and with characteristic parameters of the mixture obtained from proper mixing the characteristic parameters of pure gas and pure polymer.[17] By the coupling of the previous equation with the equilibrium conditions (equality of the chemical potentials of the gas in the gas–polymer mixture and in the pure gas phase), it is possible to evaluate the solubility of the gas in a polymer at specific temperature and pressure. In particular, if a geometric mean combination rule is assumed for the characteristic pressure, the SL–EOS is totally predictive. However, the best results in modeling sorption isotherms by the SL–EOS approach are obtained when both polymer and gas EOS parameters are determined from
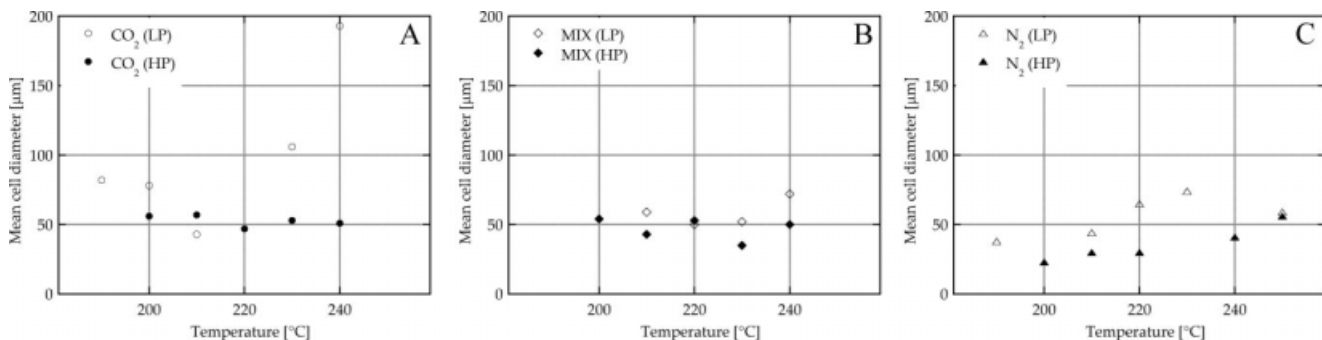
Figure 9 Mean cell diameter of the samples as function of temperature, gas type, and solubilization pressure for the CF2 polymer.
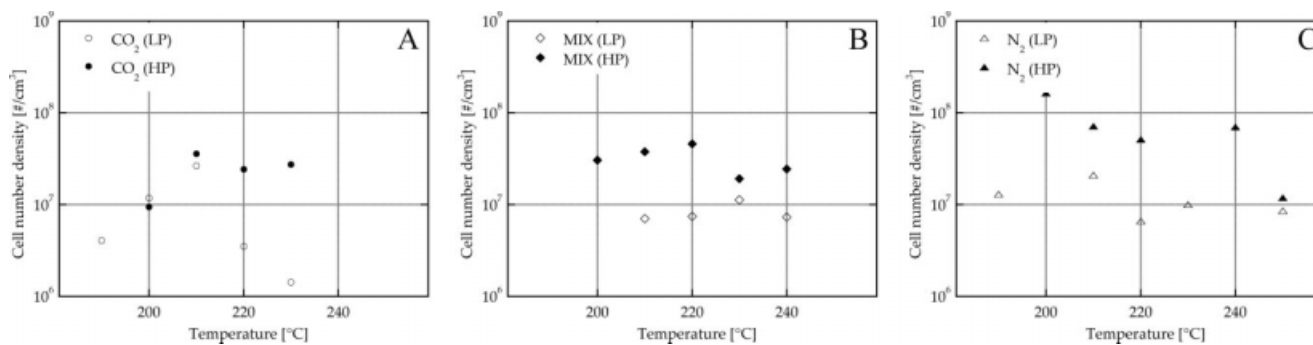
Figure 10 Cell number density of the samples as function of temperature, gas type, and solubilization pressure for the CF0 polymer.

the pure component properties in the same temperature and pressure range as for the sorption data. Furthermore, an interaction parameter (ψ) can be used as a fitting parameter of the experimental solubility data: in fact, its value is equal to 1 in the case of no interaction, whereas it is likely to be different from 1 in the case of mixture components characterized by different types of interaction energies.

Sorption thermodynamics and mass transport

Figure 5 reports the sorption isotherms of CO_2 and N_2 in CF0 at a temperature of 250°C and for pressures up to 6000 and 11,000 kPa, respectively. Typical sorption behavior was observed, with a fivefold higher solubility of carbon dioxide with respect to nitrogen. Figure 5 also reports the predicted isotherms with the SL–EOS model ($\psi = 1$); there was reasonable agreement between the data and model prediction. Figure 6 reports a typical sorption step test used to evaluate the mutual diffusivities. In particular, it was shown that, at 250°C, nitrogen/PET mutual diffusivity was more than twice the mutual diffusivity of the system containing carbon dioxide.

Batch foaming

Expansion tests were performed in a batch foaming vessel with N_2, CO_2, and an 80–20 wt % N_2–CO_2

mixture. The effects of foaming temperature, solubilization pressure, and pressure drop rate were evaluated and related to the morphological properties of the foam in terms of density, mean cell diameter, and cell number density (N_0; the number of bubbles nucleated per cubic centimeter of the original unfoamed polymer), calculated as follows:

$$N_0 = \left(\frac{n}{A}\right)^{\frac{3}{2}}\left(\frac{1}{1 - V_f}\right)$$

where

$$V_f = 1 - \frac{\rho_f}{\rho_s}$$

where V_f is the void fraction, n is the number of cells in the scanning electron microscopy (SEM) micrograph, A is the area of the micrograph (cm²), and ρ_f and ρ_s are the foam and bulk polymer densities, respectively.

All of the processing conditions are summarized in Table II. It is important to note that the bottle-grade PET, in all of the conditions used, never gave foams with reasonable densities or morphologies because they always collapsed extensively after foaming. The results of the foaming experiments on those samples are consequently not reported.

In Figure 7(A,B), the effects of the foaming temperature on the foam density are reported for CF0
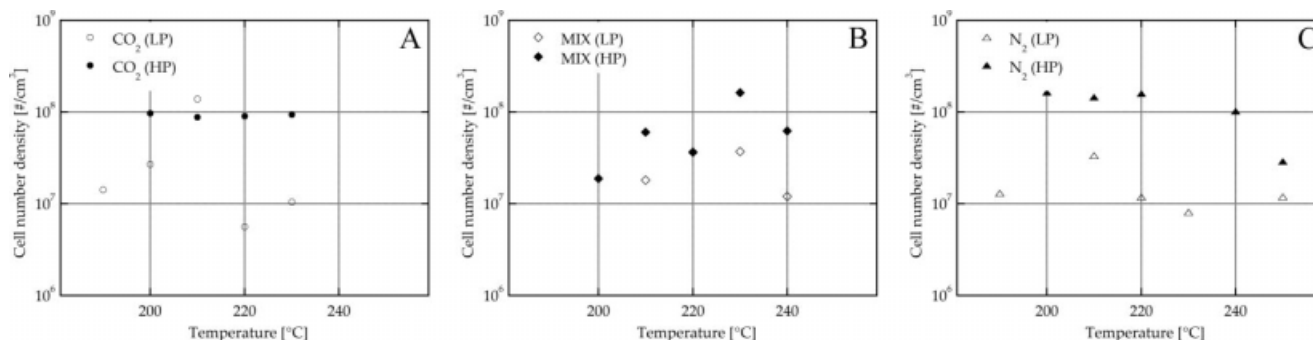
Figure 11 Cell number density of the samples as function of temperature, gas type, and solubilization pressure for the CF2 polymer.
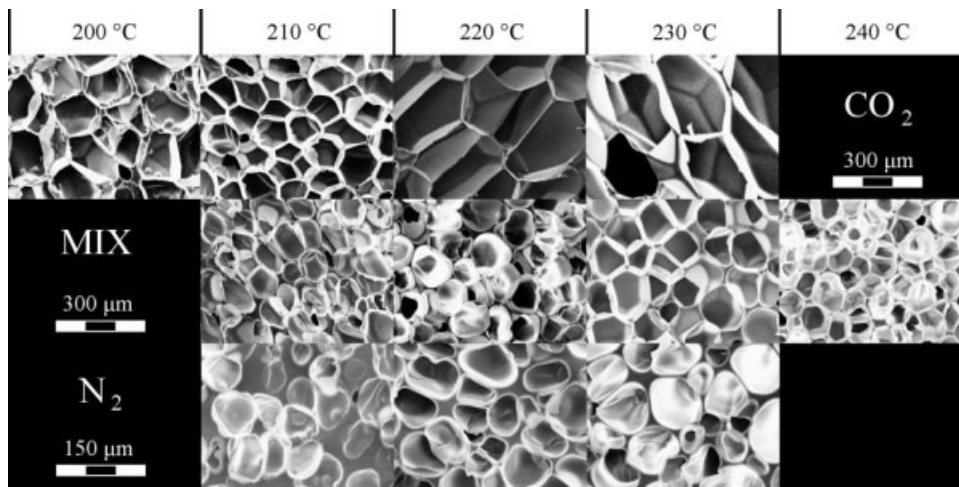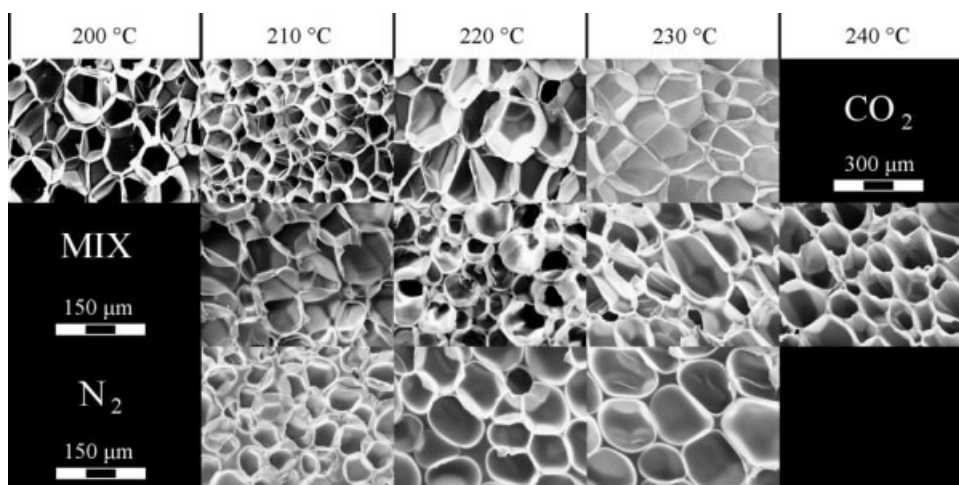
Figure 12 SEM micrographs of the CF0 foams obtained at a low solubilization pressure.

and CF2, respectively, for the LP and HP conditions. In Figure 7(A,B), the lines connecting the markers are only used to enhance the readability of data. For all of the materials, it was possible to observe a minimum temperature, below which almost bulk density was measured as a consequence of the occurrence of extensive crystallization. Conversely, above this minimum temperature, foaming was possible, and the densities decreased with increasing temperature until a minimum was achieved. Finally, at higher temperatures, the collapse of the cellular structures and, correspondingly, a densification were observed. In this way, the foaming window for each different polymer–blowing agent system was defined.

Furthermore, by comparing the curves, we found evidence that the foaming window of CF2 was 10°C shifted toward lower temperatures with respect to CF0. These results were in accordance with the thermal analysis, which proved a faster crystallization for CF0 with respect to CF2.

By analyzing the effect of the different blowing agents on densities, we observed the achievement of lower densities with CO_2 with respect to N_2, as expected from the solubility data. A temperature shift of the foaming window was also observed, which proved the higher plasticizing effect of CO_2 with respect to N_2. The mixture showed intermediate behavior, both for the temperature shift and density. By increasing the solubilization pressure to HP conditions, we achieved lower densities as a consequence of the higher amount of solubilized gas, with similar dependencies on the temperature and blowing agent type as described for the LP conditions.

Figure 8 represents the mean cell diameter of the foamed CF0 as a function of the foaming temperature for the LP and HP conditions. As shown in the figure and as expected, the mean cell diameter was strongly dependent on the solubilization pressure and the blowing agent type. As rule of thumb, it can be stated that the CO_2 produced foams were characterized by larger bubbles with respect to N_2, with

Figure 13 SEM micrographs of the CF2 foams obtained at a low solubilization pressure.
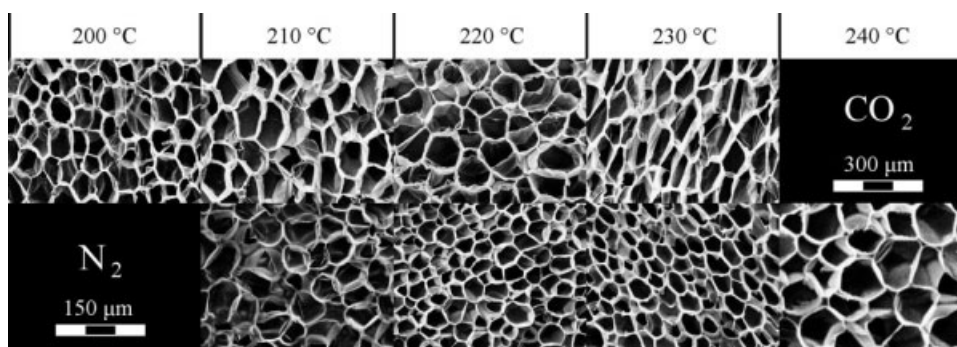
Figure 14 SEM micrographs of the CF0 foams obtained at a high solubilization pressure.

an intermediate behavior of foams produced with their mixture. As also extensively reported in the literature, an increase in gas pressure resulted in foams with reduced diameter as a consequence of the higher nucleation activity. The mean cell diameter slightly increased with temperature for all three blowing agents. This behavior was related to the reduction in polymer viscosity with temperature. Similar conclusions were drawn for the CF2 samples, whose results are reported in Figure 9. The main difference was the lower values of mean cell diameters exhibited by the CF2 samples for all blowing agents and foaming temperatures.

Figures 10 and 11 report the cell number density of the CF0 and CF2 foams, respectively, as function of foaming temperature and pressure for all of the different blowing agents. As already shown in Figures 8 and 9, the main effect of saturation pressure was the enhanced bubble nucleation with the increasing saturation pressure, as evidenced by the raised cell number densities at different temperatures. Moreover, N_2 was much more effective in bubble nucleation with respect to CO_2, whereas an intermediate behavior was shown by the mixture. Those data were in agreement with data reported on polycaprolactone (PCL).[20]

At 200°C and HP, we produced foams with a mean diameter of 30 μm and a foam density of 0.20 g/cm^3 with N_2 and foams with a mean diameter of about 50 μm and a foam density of 0.06 g/cm^3 with CO_2. In both cases, the cell number density was about 10^8 cm^{-3}.

SEM micrographs of foams with approximately the same density of 0.06 g/cm^3 are shown in Figures 12–15. As evident, the morphologies of the foams were strongly dependent on the foaming temperature and solubilization pressure.

As the degree of undercooling increased (i.e., the difference between the polymer melting temperature and the foaming temperature), the cell diameters decreased until a minimum was reached, and then, the cell diameters increased again. This behavior was common to all of the used gases and was related to the competing effect of the nucleation of new bubbles (higher and higher with the degree of undercooling) and the diffusion of gas in the nucleated cells (the higher the temperature was, the higher this effect was). At temperatures below the minimum peak, the behavior was dominated by the viscous properties, and even if a higher number of cells were nucleated, only a few of them were able to grow.

At higher solubilization pressures, this behavior was still present, but the morphology was finer. Under these conditions, in fact, the nucleation was also strongly influenced by the thermodynamic instability increase related to the higher amount of gas solubilized and the enhanced pressure drop rate. This resulted in foams with a higher number of cell nucleated at each temperature, with lower density and smaller cell dimensions.

In general, with regard to the batch expansion of these two foam-grade PETs, we can state that, by
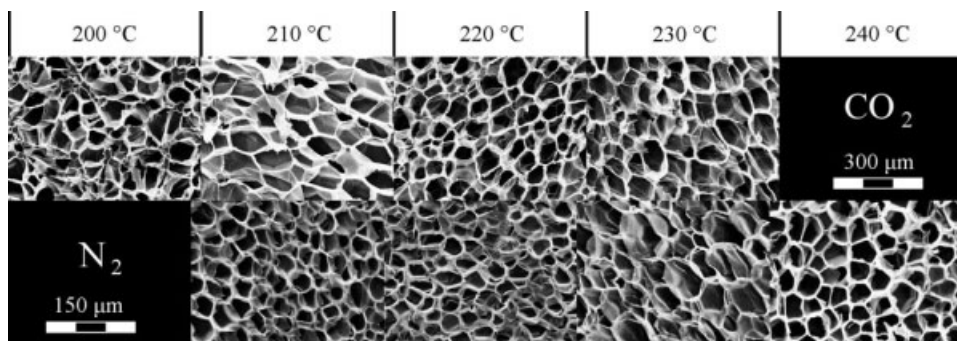
Figure 15 SEM micrographs of the CF2 foams obtained at a high solubilization pressure.

comparing Figures 7(A) and 10 for CF0 and 7(B) and 11 for CF2, the CO_2 seemed to be a better blowing agent, for it allowed us to strongly reduce the foam density (with densities as low as 0.06 g/cm^3) and to obtain a fine morphology when a high solubilization pressure was used.

CONCLUSIONS

The foaming windows of two high-molecular-weight PETs (an homopolymer and a copolymer) were determined as a function of gas type (CO_2, N_2, and a 80/20 wt % mixture of N_2/CO_2), foaming temperature, solubilization pressure, and pressure drop rate. These properties were correlated to the thermal, rheological, volumetric, and gas sorption properties. Thermal analysis showed that the homopolymer PET exhibited the onset temperature of crystallization that defined the lowest foaming temperature, 10°C higher than that of the copolymer. The SL–EOS was used to predict the gas sorption properties in the molten state of the investigated polymers. The reduced parameters needed for SL–EOS were evaluated by dilatometric pVT analysis, and predictions were corrected by means of the solubility parameter. The mass gas sorption of CO_2 was found to be fivefold that of N_2; on the contrary, the diffusivity coefficient of N_2 was much higher than that of carbon dioxide. Foaming experiments, performed with a batch process, showed that densities as low as 0.06 g/cm^3 could be obtained with CO_2 as a blowing agent because of its higher solubility, whereas the use of N_2 or the mixture induced densities as low as 0.16 g/cm^3. The effect of the higher diffusivity of N_2 resulted in an increase in cell density and a reduction in cell diameter, in particular, at a high solubilization pressure, with a cell diameter as low as 25 μm and a cell number density higher than 10^8 cells/cm^3.

References

1. Iroh, J. O. In Polymer Data Handbook; Mark, J. E., Ed.; Oxford University Press: New York, 1999.
2. Guan, R.; Wang, B.; Lu, D. J App Polym Sci 2003, 88, 1956.
3. Japon, S.; Boogh, L.; Leterrier, Y.; Månson, J.-A. E. Polymer 2000, 41, 5809.
4. Haralabakopoulos, A. A.; Tsiourvas, D.; Paleos, C. M. J Appl Polym Sci 1999, 71, 2121.
5. Incarnato, L.; Scarfato, P.; Di Maio, L.; Acierno, D. Polymer 2001, 41, 6825.
6. Forsythe, J. S.; Cheah, K.; Nisbet, D. R.; Gupta, R. K.; Lau, A.; Donovan, A. R.; O'Shea, M. S.; Moad, G. J Appl Polym Sci 2006, 100, 3646.
7. Xanthos, M.; Wan, C.; Dhavalikar, R.; Karayannidis, G. P.; Bikiaris, D. N. Polym Int 2004, 53, 1161.
8. Al Ghatta, H.; Severini, T. J Eng Appl Sci 1996, 2, 1846.
9. Al Ghatta, H.; Cobror, S. U.S. Pat. 5,776,994 (1998).
10. Hirai, T.; Amano, N. Proc. 51st SPE ANTEC, 1993, 36, 1256.
11. Baldwin, D. F.; Park, C. B.; Suh, N. P. Polym Eng Sci 1996, 36, 1437.
12. Baldwin, D. F.; Park, C. B.; Suh, N. P. Polym Eng Sci 1996, 36, 1446.
13. Zoeller, P.; Bolli, P.; Pahud, V.; Ackerman, H. Rev Sci Instrum 1976, 47, 948.
14. Sorrentino, L.; Iannace, S.; Di Maio, E.; Acierno, D. J Polym Sci Part B: Polym Phys 2005, 43, 1966.
15. Spitael, A. P.; Macosko, C. W. Polym Eng Sci 2004, 44, 2090.
16. Sanchez, I. C.; Lacombe, R. H. J Phys Chem 1976, 80, 2352.
17. Sanchez, I. C.; Lacombe, R. H. Macromolecules 1978, 2, 1145.
18. Wang, N.-H.; Ishida, S.; Takishima, S.; Masuoka, H. Kagaku Kogaku Ronbunshu 1992, 18, 226.
19. Wang, N.-H.; Hattori, K.; Takishima, S.; Masuoka, H. Kagaku Kogaku Ronbunshu 1991, 17, 1138.
20. Di Maio, E.; Mensitieri, G.; Iannace, S.; Nicolais, L.; Li, W.; Flumerfelt, R. W. Polym Eng Sci 2005, 45, 432.